Jorgensen, C. K., & Judd, B. R. (1964) *Mol. Phys. 8*, 281–290.
Matthews, B. W., & Weaver, L. H. (1974) *Biochemistry 13*, 1719–1725.
Matthews, B. W., Colman, P. M., Jansonius, J. N., Titani, K., Walsh, K. A., & Neurath, H. (1972) *Nature (London), New Biol. 238*, 41–43.
Matthews, B. W., Weaver, L. H., & Kester, W. R. (1974) *J. Biol. Chem. 249*, 8030–8044.
Nakazawa, E., & Shionoya, S. (1967) *J. Chem. Phys. 47*, 3211–3219.
Ohta, Y., Ogura, Y., & Wada, A. (1966) *J. Biol. Chem. 241*, 5919–5925.
Reisfeld, R. (1975) *Struct. Bonding (Berlin) 22*, 123–174.
Reisfeld, R. (1976) *Struct. Bonding (Berlin) 30*, 65–98.
Rhee, M.-J., Sudnick, D. R., Arkle, V. K., & Horrocks, W. DeW., Jr. (1981) *Biochemistry* (preceding paper in this issue).
Roche, R. S., & Voordouw, G. (1978) *CRC Crit. Rev. Biochem. 5*, 1–23.
Stein, G., & Wurzberg, E. (1975) *J. Chem. Phys. 62*, 208–213.
Steinberg, I. Z. (1971) *Annu. Rev. Biochem. 40*, 83–114.
Stryer, L. (1978) *Annu. Rev. Biochem. 47*, 819–846.
Sudnick, D. R. (1979) Ph.D. Thesis, The Pennsylvania State University, University Park, PA.
Titani, K., Hermodson, M. A., Ericsson, L. H., Walsh, K. A., & Neurath, H. (1972) *Nature (London), New Biol. 238*, 35–37.
Woyski, M. M., & Harris, R. E. (1963) in *Treatise on Analytical Chemistry* (Kolthoff, I. M., & Elving, P. J., Eds.) Part 2, Vol. 8, p 58, Wiley, New York.

# Resonance Raman and Absorption Spectroscopic Detection of Distal Histidine–Fluoride Interactions in Human Methemoglobin Fluoride and Sperm Whale Metmyoglobin Fluoride: Measurements of Distal Histidine Ionization Constants†

Sanford A. Asher,* Mary L. Adams, and Todd M. Schuster

ABSTRACT: The pH dependence of the resonance Raman and absorption spectra of human methemoglobin fluoride ($Hb^{III}F$) and sperm whale metmyoglobin fluoride ($Mb^{III}F$) has been examined. Both the Raman and absorption spectra of $Hb^{III}F$ and $Mb^{III}F$ indicate the existence at alkaline pH of an equilibrium between the hydroxide and fluoride complexes. The absorption maxima of $Hb^{III}F$ and $Mb^{III}F$ solutions shift to longer wavelengths as the pH is decreased from neutrality. The Raman data show a corresponding shift of the 461- and 468-$cm^{-1}$ Fe–F vibrational stretching peaks at pH 7.0 [Asher, S. A., & Schuster, T. M. (1979) *Biochemistry 18*, 5377] to 399 and 407 $cm^{-1}$ at acid pH in $Mb^{III}F$ and $Hb^{III}F$, respectively. These shifts are interpreted to result from protonation of the distal histidine and the formation of a hydrogen bond to the fluoride ligand. Measurements of the pH dependence of the absorption and resonance Raman spectra give distal histidine ionization constants (apparent) corresponding to p$K$ = 5.1 (±0.1) for $Hb^{III}F$ and p$K$ = 5.5 (±0.1) for $Mb^{III}F$. An examination of the distal histidine p$K$ values and the frequency of the hydrogen-bonded Fe–F stretching vibration at pH 5.0 of $Hb^{III}F$ with and without inositol hexaphosphate indicates little difference in the distal histidine–heme distance between the so-called R and T quaternary forms of $Hb^{III}F$. These results indicate that the changes in the electronic spectrum of $Hb^{III}F$ that occur upon switching from the R to the T form do not result from alterations in (1) the iron–fluoride bond distance, (2) the iron out-of-heme plane distance, or (3) the distal histidine–fluoride distance.

Hemoglobin cooperativity depends upon the modulation of heme–ligand affinity by the globin portion of the molecule in response to binding at other sites on the protein. One approach that has been taken to elucidate the mechanism of cooperativity in hemoglobin has been to study the structural changes in the ferric derivatives of hemoglobin which are brought about by the binding of allosteric effectors [for recent reviews, see Perutz (1979) and Moffat et al. (1979)]. The quaternary structure of methemoglobin fluoride ($Hb^{III}F$)[1] is that of the liganded ferrous derivative, the so-called "R structure" (Deatherage et al., 1976), whereas in the presence of inositol hexaphosphate ($InsP_6$) it assumes the "T structure" of deoxyhemoglobin (Fermi & Perutz, 1977). This structural change gives rise to changes in SH reactivity and UV, visible, CD, and proton NMR spectra (Perutz et al., 1974a–c, 1978) which appear to be diagnostic for similar R–T conversions in other hemoglobin derivatives.

In an effort to define this R–T structural change in terms of bonding changes, we have used resonance Raman spectroscopy to study accompanying changes of iron spin state, iron–axial ligand bonding, and heme geometry (Asher et al., 1977; Asher & Schuster, 1979, 1981a,b). A central conclusion of those studies was that the iron–fluoride bond distance does not change when methemoglobin fluoride is switched from the R to the T conformation. Here, we report on an examination

† From the Gordon McKay Laboratory, Division of Applied Sciences, Harvard University, Cambridge, Massachusetts 02138 (S.A.A.), and the Biochemistry and Biophysics Section, Biological Sciences Group, University of Connecticut, Storrs, Connecticut 06268 (M.L.A. and T.M.S.).
*Received November 12, 1980.* This work was supported by National Institutes of Health Grants GM-24081 (to P. S. Pershan) and HL-24644 and National Science Foundation Grant PCM 79-03964 (to T.M.S.).
* Address correspondence to this author at the Department of Chemistry, University of Pittsburgh, Pittsburgh, PA 15260.

[1] Abbreviations used: $Hb^{III}F$, methemoglobin fluoride; $Mb^{III}F$, metmyoglobin fluoride; $InsP_6$, inositol hexaphosphate; Hepes, *N*-2-(hydroxyethyl)piperazine-*N*′-2-ethanesulfonic acid.

0006-2960/81/0420-3339$01.25/0 

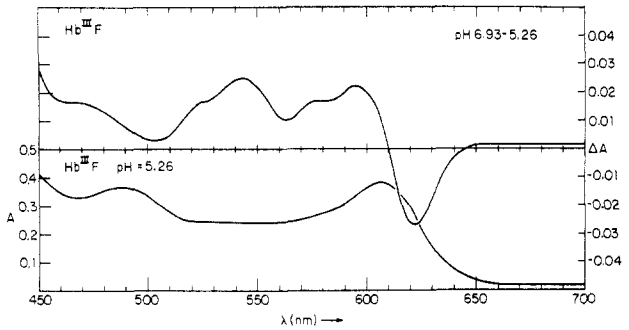


FIGURE 1: Absorption and pH difference spectrum (pH 6.93–5.26) for methemoglobin fluoride. Absorption spectrum shown is for a pH 6.93 sample. $Hb^{III}F$ concentration = 42 $\mu$M heme, 0.1 M KF, and 0.025 M buffer ($KPO_4^{2-}$, pH 6.93, and sodium acetate, pH 5.26). Path length = 1 cm; $T$ = 20 °C. Spectral bandwidth is <1 nm at 540 nm and <1.5 nm at 630 nm.

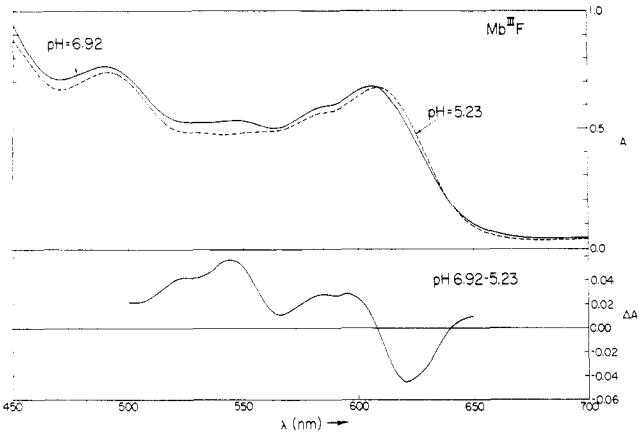


FIGURE 2: Absorption and pH difference spectrum (pH 6.92–5.23) for metmyoglobin fluoride. $Mb^{III}F$ concentration = 87 $\mu$M heme. Other conditions as in Figure 1.

of direct interactions between the iron-bound fluoride ligand and the distal histidine (E7) in the fluoride derivatives of human methemoglobin ($Hb^{III}F$) and sperm whale metmyoglobin ($Mb^{III}F$).

## Experimental Procedures

Human hemoglobin $A_0$ and sperm whale myoglobin, fraction IV, were purified as previously described (Asher & Schuster, 1979, 1981a,b), and unbuffered stock solutions were prepared from aquomethemoglobin and lyophilized metmyoglobin in doubly distilled water. The $Hb^{III}F$ and $Mb^{III}F$ sample solutions at different pH values were prepared by diluting the appropriate volume of stock solution into a buffer solution which contained KF close to the final desired pH value.

Measurements of pH were made by using either an Orian 701 A meter and 91-02 combination microelectrode or a Radiometer PHM-64 meter and GK2322C combination electrode. The presence of KF in buffers can interfere with pH measurements, and this was observed as a drift in the readings after about 1–2 min. Therefore, the values reported are those obtained as soon as a stable reading was obtained but before drift could be detected, i.e., 15–30 s after the calibrated electrode was placed in the KF-containing final heme protein solution. Repeated measurements of a solution in this manner resulted in a measuring precision of ±0.03 pH unit, slightly less than the calibration accuracy of ±0.02 pH unit. Inositol hexaphosphate was added to hemoglobin solutions as a concentrated buffered solution or as dry crystals. Absorption spectra were recorded by using a Cary 118C (Varian Instruments) spectrophotometer interfaced to a Nova computer. Difference absorption spectra were obtained by direct digital subtraction of base-line-corrected spectra. Measurements were made by using specially designed thermostated cell holders which provide temperature uniformity of ±0.05 °C throughout the cell. The Raman spectra were measured by using a microcomputer-interfaced Raman spectrometer described in detail elsewhere (Asher & Schuster, 1979). A rotating sample cell was used to avoid thermal decomposition or photoreduction of the sample. The Raman difference spectra were obtained by direct numerical subtraction of the original data.

## Results

The absorption spectra of $Hb^{III}F$ and $Mb^{III}F$ solutions near pH 5 and 7 and the corresponding pH difference spectra are shown in Figures 1 and 2, respectively. Both sets of spectra display broad features in the 4500–7000-Å spectral region with distinct absorption maxima at 6000–6100 Å. Magnetic circular dichroism (MCD) and single-crystal absorption measurements indicate that the broad absorption spectra result from a complex superposition of numerous absorption bands which presumably result from admixtures of $\pi \rightarrow \pi^*$ and charge-transfer electronic transitions (Eaton & Hochstrasser, 1968; Zerner et al., 1966; Smith & Williams, 1970; Vickery et al., 1976; Churg et al., 1980).

A pronounced pH dependence is observed for the absorption spectra of both $Hb^{III}F$ and $Mb^{III}F$ above pH 7, where the spectra are indicative of formation of the hydroxide derivatives (not shown) as previously observed by Theorell & Ehrenberg (1951) and by Fabry & Eisenstadt (1974). NMR data also indicate the presence of an equilibrium between $Mb^{III}OH$ and $Mb^{III}F$, and of $Hb^{III}OH$ and $Hb^{III}F$ at alkaline pH (Gupta & Mildvan, 1975; Fabry & Eisenstadt, 1974).

As the pH is lowered to values below pH 7.0, the absorption maxima shift to longer wavelengths (red shifts) as shown in Figures 1 and 2. The pH difference spectra in Figures 1 and 2 show characteristic maxima, minima, and isosbestic points for $Mb^{III}F$ and $Hb^{III}F$ which are summarized in Table I. Data not shown in Table I indicate that the pH difference spectra do not result from substitution of $OH^-$ by $F^-$. The absorption difference spectra are also not consistent with the replacement of fluoride by water. Replacement of the $F^-$ ligand by a water molecule at low pH would result in a 640–650-nm minimum in the difference spectra if either $Mb^{III}HOH$ or $Hb^{III}HOH$ were forming (see Table I). Furthermore, the isosbestic points of the pH difference spectra clearly indicate that the aquo complexes are not being formed as the pH changes from 7 to 5. In addition, the dissociation constant for the reaction $H_2O$ + $Hb^{III}F$ ($Mb^{III}F$) $\rightleftarrows$ $Hb^{III}HOH$ ($Mb^{III}HOH$) + $F^-$ *decreases* with decreasing pH, indicating that increased $F^-$ binding occurs as the pH is decreased (Theorell & Ehrenberg, 1951; Beetlestone & Irvine, 1968, 1969). Thus, these pH-dependent spectral changes may reflect either alterations in the heme geometry or changes in the interactions of the heme and its ligands with the globin, but not changes in the identity of the sixth ligand.

As shown in Figures 3 and 4, the resonance Raman spectra of $Mb^{III}F$ and $Hb^{III}F$ demonstrate a more dramatic pH dependence. Each of the Raman spectra displays peaks at ca. 760, 1550, and 1610 $cm^{-1}$ in addition to the 983-$cm^{-1}$ peak resulting from $SO_4^{2-}$ added to the samples in the form of $Na_2SO_4$ as an intensity and frequency standard. The peaks above 600 $cm^{-1}$ previously assigned to in-plane porphyrin macrocyclic vibrational modes show little or no dependence upon sample pH; the 1550- and 1610-$cm^{-1}$ peaks are the spin state sensitive modes, indicating a high-spin iron (Spiro &

Table I: Spectral Characteristics of $Mb^{III}F$ and $Hb^{III}F$[a]

| | maxima (nm) | minima (nm) | isosbestics (nm) (difference spectra) |
|---|---|---|---|
| $Mb^{III}F$; pH 6.92, 25 mM $K(H)PO_4$ | 607 | 564 | |
| | 583 | 470 | |
| | 547 | | |
| | 490 | | |
| $Mb^{III}F$; pH 5.23, 25 mM acetate | 609 | 560 | |
| | 583 | 470 | |
| | 491 | | |
| $Mb^{III}F$ (pH 6.92–5.23) | 595 | 620 | 608 |
| | 585 | 565 | |
| | 545 | | |
| | 470 | | |
| $Mb^{III}F$-$Mb^{III}HOH$; pH 6.0, 100 mM $K(H)PO_4$ | 607 | 648 | 633 |
| | 478 | 513 | 539 |
| | | | 492 |
| $Hb^{III}F$; pH 6.93, 50 mM $K(H)PO_4$ | 606 | 562 | |
| | 546 | 467 | |
| | 487 | | |
| $Hb^{III}F$; pH 5.26, 25 mM acetate | 607 | 540 | |
| | 489 | 467 | |
| $Hb^{III}F$ (pH 6.93–5.26) | 595 | 622 | 610 |
| | 578 | 567 | |
| | 543 | 506 | |
| | 525 | | |
| $Hb^{III}F$-$Hb^{III}HOH$; pH 6.0, 100 mM $K(H)PO_4$ | 605 | 640 | 629 |
| | | 511 | 536 |
| | | | 493 |
| $Hb^{III}F \pm InsP_6$; pH 6.93, 25 mM $K(H)PO_4$ | 626 | 597 | 614 |
| | 560 | 549 | 534 |
| | 508 | 475 | 489 |
| $Hb^{III}F \pm InsP_6$; pH 5.26, 25 mM $K(H)PO_4$ | 628 | 597 | 614 |
| | 508 | 475 | 541 |
| | | | 489 |

[a] All measurements were made at 20 °C in 0.10 M KF plus the indicated buffer. These data have not been corrected for the small increases in fluoride association constants which occur as the pH decreases (Beetlestone & Irvine, 1968).

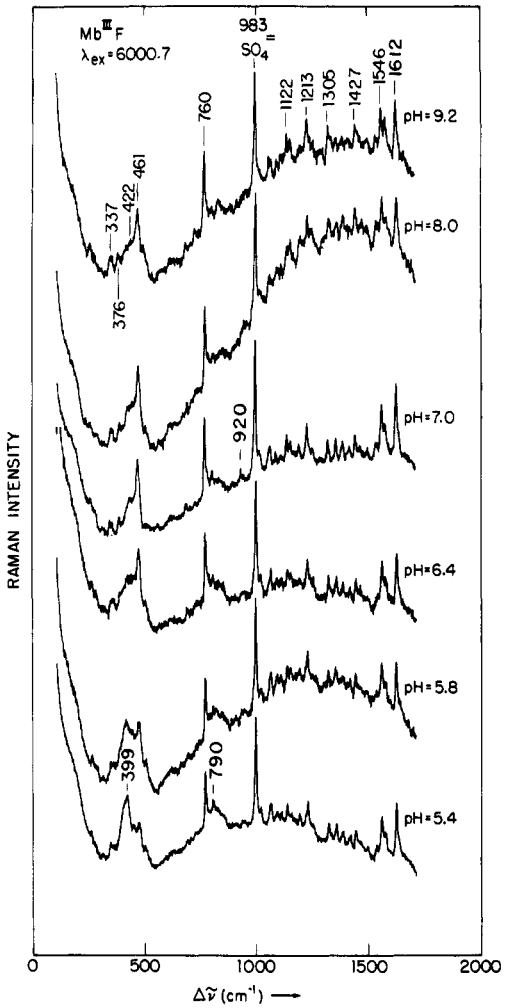


FIGURE 3: pH dependence of $Mb^{III}F$ resonance Raman spectra. $\lambda_{ex}$ = 6000.7 Å; laser power = 0.37 W; integration time = 1 s; average slit width = 4 $cm^{-1}$. Heme concentration was ca. 0.18 mM in 0.2 M Hepes, 0.2 M $Na_2SO_4$, 0.1 M KF, and 1.0 mM EDTA; $T$ = 22 °C.

Burke, 1976; Spiro, 1975; Kitagawa et al., 1976).

Iron–axial ligand vibrational stretching modes occur below 600 $cm^{-1}$ upon excitation within charge-transfer absorption bands (Asher & Sauer, 1976); the 461- and 422-$cm^{-1}$ peaks in $Mb^{III}F$ and 468 and 439 $cm^{-1}$ in $Hb^{III}F$ have been assigned to FeF stretching vibrations (Asher et al., 1977; Asher & Schuster, 1979, 1981a,b). The relative intensities of the two Fe–F stretching Raman peaks in each protein depend on the excitation wavelength (Asher et al., 1977). The 461- and 468-$cm^{-1}$ peaks result from diatomic Fe–F stretches, while the 422- and 439-$cm^{-1}$ peaks were interpreted to result from Fe–F vibrations lowered in frequency because of hydrogen bonding of the fluoride ion to a water molecule (Asher et al. 1977; Asher & Schuster, 1979, 1981a,b) which has been shown to be present in some of the heme cavities in crystals (Deatherage et al., 1976) and in solution (Koenig et al., 1981). At pH 9.2, a shoulder on the high-frequency side of the 461-$cm^{-1}$ peak at ca. 490 $cm^{-1}$ occurs in $Mb^{III}F$ (Figure 3), presumably reflecting the presence of the hydroxide complex of $Mb^{III}$ in which the Fe–O stretch occurs at 490 $cm^{-1}$ (Asher & Schuster, 1979). No changes are observed in the 1500–1700-$cm^{-1}$ Raman spin state sensitive region with excitation at ca. 6000 Å, because this excitation wavelength enhances only the high-spin species of the $Mb^{III}OH$ spin-state equilibrium; the high-spin Raman peaks of $Mb^{III}OH$ occur at essentially the same frequencies as do the 1546- and 1612-$cm^{-1}$ peaks of $Mb^{III}F$ (Asher & Schuster, 1979). The presence of an equilibrium between $Mb^{III}OH$ and $Mb^{III}F$ at high pH, noted earlier by NMR and absorption measurements in horse $Mb^{III}F$ and human $Hb^{III}F$, indicates an apparent p$K$ value of ca. 10 for equal mixtures of $Mb^{III}F$ and $Mb^{III}OH$ in horse $Mb^{III}F$ (Theorell & Ehrenberg, 1951; Fabry & Eisenstadt, 1974) and an apparent p$K$ of 8.5 in human $Hb^{III}F$ (Gupta & Mildvan, 1975).

As the pH is decreased from neutrality, a decrease in intensity occurs for the 461- ($Mb^{III}F$) and 468-$cm^{-1}$ ($Hb^{III}F$) Fe–F stretching vibrations in conjunction with the appearance of 399- ($Mb^{III}F$) and 407-$cm^{-1}$ ($Hb^{III}F$) peaks. Due to the breadth of the 399-$cm^{-1}$ peak in $Mb^{III}F$ and the 407-$cm^{-1}$ peak in $Hb^{III}F$, it is difficult to determine whether the intensities of the water hydrogen-bonded Fe–F stretch at 422 $cm^{-1}$ in $Mb^{III}F$ and at 439 $cm^{1}$ in $Hb^{III}F$ also decrease in intensity as the pH decreases.

The Raman pH difference spectra shown in Figures 5 and 6 for $Mb^{III}F$ and $Hb^{III}F$ graphically display these pH-dependent Raman spectral changes. The pH difference spectrum between the pH 8.0 and pH 5.4 $Mb^{III}F$ samples (Figure 5) is completely devoid of features except for the peak and trough at 461 and 399 $cm^{-1}$, respectively. A small trough at ca. 790 $cm^{-1}$ indicates the appearance of a new Raman peak in $Mb^{III}F$ at low pH. The $Hb^{III}F$ difference spectrum (Figure 6) shows similar features, with a peak and trough at 461 and 407 $cm^{-1}$ and a trough at ca. 800 $cm^{-1}$. In addition, a decreased intensity for the peak at 758 $cm^{-1}$ in $Hb^{III}F$ at low pH is evident from the peak in the difference spectrum.

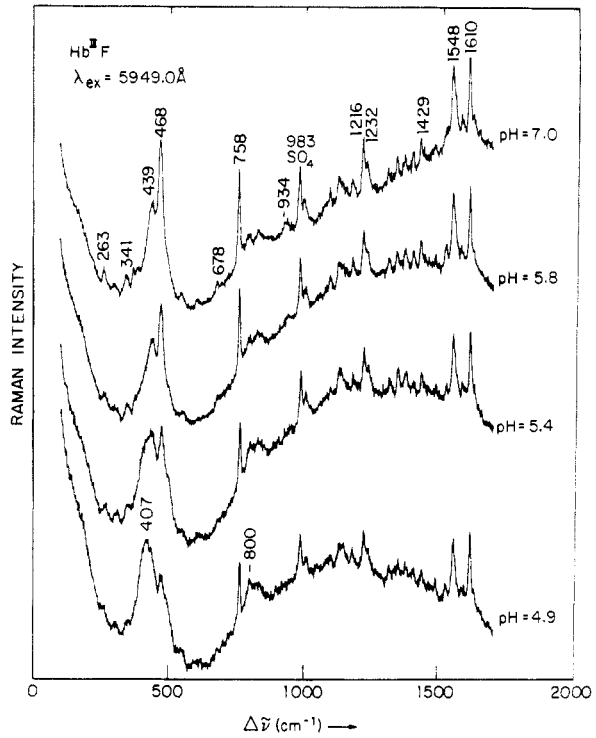


FIGURE 4: pH dependence of resonance Raman spectra of $Hb^{III}F$. $\lambda_{ex}$ = 5949.0 Å; power = 0.25 W; integration time = 1 s; average slit width = 4 $cm^{-1}$. Heme concentration = 0.31 mM in 0.04 M $Na_2SO_4$ and 0.08 M KF. pH 7 sample, 0.041 M Hepes; pH 5.8 sample, 0.04 M $Na_2PO_4$; pH 5.4 and 4.90 samples, 0.04 M sodium acetate; $T$ = 22 °C.

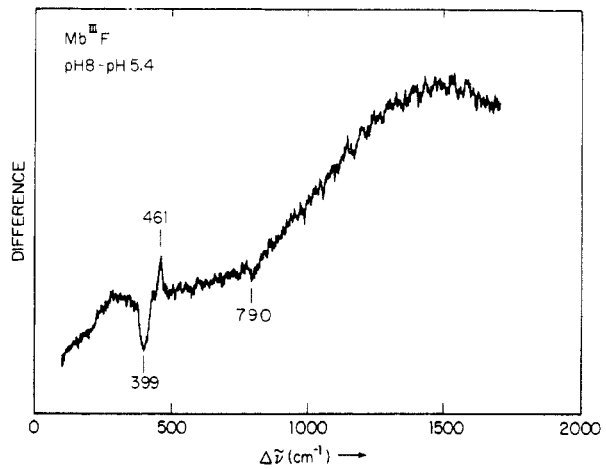


FIGURE 5: pH difference $Mb^{III}F$ Raman spectrum between pH 8 and 5.4. Individual spectra shown in Figure 3.

The fact that no changes in peak positions (±1 $cm^{-1}$) or intensities (±10%) occur for any of the heme macrocyclic vibrational modes, in contrast to the dramatic changes seen in the axial ligand vibrational modes, is strongly indicative of changes in fluoride bonding. As was concluded from the previously discussed absorption spectral data, it is unlikely that the Raman spectral changes result from substitution of the fluoride ligand by water in the heme cavity because the iron remains high spin (no changes occur in the spin-state Raman peaks at 1546 and 1609 $cm^{-1}$) and the absorption spectral changes are small and not characteristic of $\pm F^-$ difference spectra (see Table I). Also, the characteristic high-spin aquo Raman peak at 1615 $cm^{-1}$ is not seen, and the 399-$cm^{-1}$ peak in $Mb^{III}F$ is not observed in $Mb^{III}H_2O$ upon excitation between 5800 and 6300 Å (S. A. Asher and T. M. Schuster, unpublished experiments).

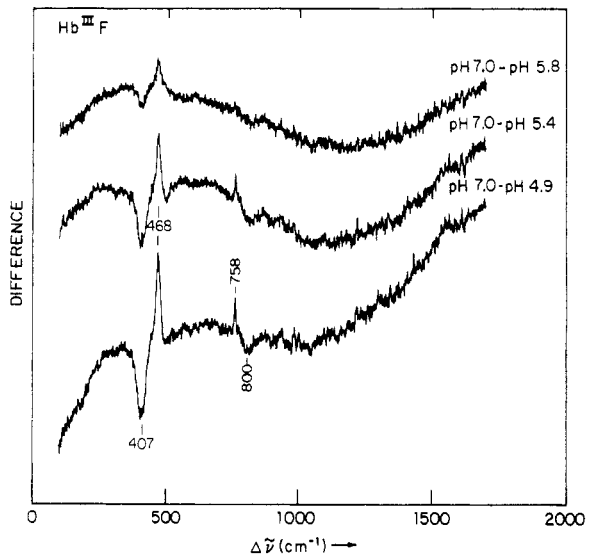


FIGURE 6: pH difference $Hb^{III}F$ Raman spectra from Figure 4 data.

The changes in the absorption and resonance Raman spectra are continuous with pH, and Figure 7 shows the absorption and resonance Raman spectra titration curves for $Hb^{III}F$ and $Mb^{III}F$. The absorption spectral data are plotted as changes in extinction at 5400 Å. As shown in the pH difference absorption spectra, the 5400-Å absorption spectral changes parallel those occurring in the 6000-Å absorption band. The Raman spectral data are plotted in Figure 7 as the intensity of the 461-$cm^{-1}$ peak scaled such that the 461-$cm^{-1}$ peak intensity is equal to 1.0 at pH 7.0. Also shown are points calculated from the intensity of the 399-$cm^{-1}$ peak. The magnitudes of the peak and trough in the $Mb^{III}F$ Raman difference spectra are not equal; as a result, the 399-$cm^{-1}$ peak intensity was normalized by a factor equal to the intensity of the 461-$cm^{-1}$ peak divided by the intensity of the 399-$cm^{-1}$ trough. The data are plotted as 1.0 minus the normalized 399-$cm^{-1}$ peak intensity. For $Hb^{III}F$, the peak and trough intensities are equal (Figure 6). Thus, the 468-$cm^{-1}$ Raman peak intensity was plotted such that the 468-$cm^{-1}$ peak intensity at pH 7.0 was set equal to 1.0.

Figure 7 also shows theoretical titration curves by using the Henderson–Hasselbalch equation for various (indicated) p$K$ values. The data were fit to a linearized form of the Henderson–Hasselbalch equation by using an unweighted linear least-squares minimization routine but fixing the alkaline end point at pH 7 in each case. This procedure provided the best-fit acid end-point values of the extinctions and the apparent p$K$ values. Correlation coefficients of 0.98 were obtained for a fit to a single titrating group in each case. Within the accuracy of our titration data, we cannot resolve different p$K$ values for the $\alpha$ and $\beta$ subunits. Both the absorption and resonance Raman $Mb^{III}F$ and $Hb^{III}F$ titration data graphically appear consistent with single p$K$ titrations of some species with an apparent p$K$ = 5.5 ± 0.1 for $Mb^{III}F$ and p$K$ = 5.1 ± 0.1 for $Hb^{III}F$. The absorption and resonance Raman titration data at alkaline pH do not lie on the calculated titration curves because of the competitive binding of $OH^-$ above about pH 7.5.

We propose that the ca. 60-$cm^{-1}$ Raman shift of the Fe–F stretching vibration to lower frequency in both $Mb^{III}F$ and $Hb^{III}F$ at low pH results from protonation of the distal histidine and an accompanying formation of a hydrogen bond to the $F^-$ anion, thereby decreasing the Fe–F force constant. Our assignments for the Raman doublet and the pH-dependent spectral shifts are shown in Figure 8. Figure 8a indicates the

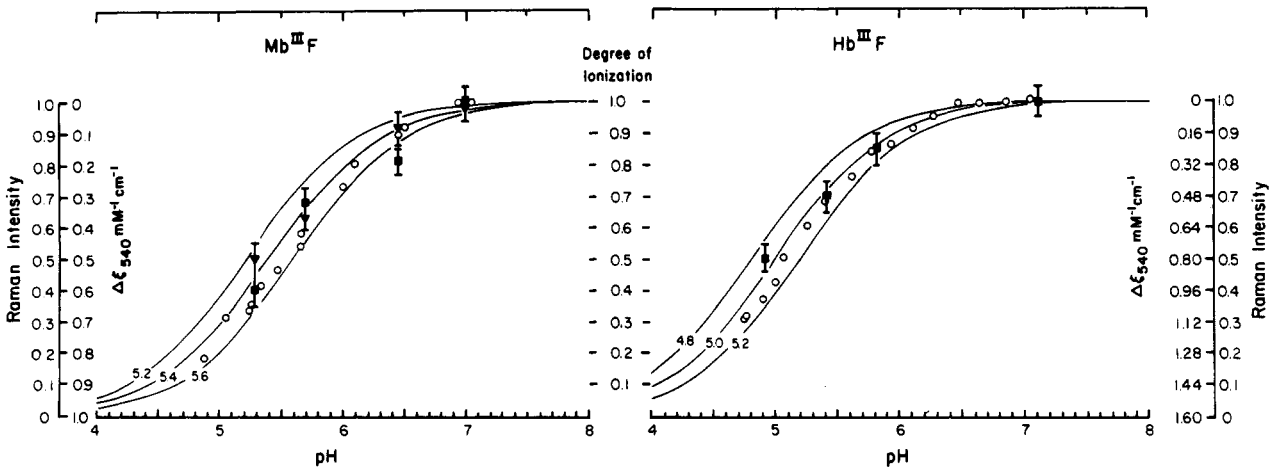


FIGURE 7: pH dependence of the absorption spectra monitored at 540 nm (○) and the intensity of the 461- (▼) and 399-cm$^{-1}$ (■) Fe stretching Raman peaks of $Mb^{III}F$ and the 468- and 407-cm$^{-1}$ (■) Fe–F stretching Raman peaks of $Hb^{III}F$. Also shown are representative pH titration curves calculated from the Henderson–Hasselbalch equation. See text for details.

partial occupancy of water in some of the heme crevices at neutral pH by indicating the $H_2O$ as dashes. We presume that this water molecule bridges the distal histidine and the fluoride ligand. At low pH values, the $N_\epsilon$ of the distal histidine protonates and hydrogen bonds directly to the $F^-$ (Figure 8b).

Fabry & Eisenstadt (1974) in NMR studies of horse $Mb^{III}F$ also observe a titration of a group in the heme crevice which changes the optical and proton relaxation behavior of $Mb^{III}F$ solutions. However, in their titration, they observe a p$K$ of ca. 6.0 which they ascribe to protonation of the proximal histidine. This mechanism appears unlikely because protonation of the proximal histidine must result in an increased positive charge at the iron. Since the Fe–F is ionically bound, the force constant would *increase* linearly with charge at the iron, rather than decrease as is observed.

Our assignment of distal histidine protonation and hydrogen bonding is consistent with an extensive literature on the pH dependence of $^{13}C$, $^{15}N$, and proton NMR spectra of various Mb derivatives. For example, the $^{13}C$ NMR studies of horse $Mb^{III}CN$ indicate a p$K$ value of 5.3 for either the proximal or the distal histidine (Wilbur & Allerhand, 1977) while $^{13}CO$ NMR studies of sperm whale and horse $Mb^{II}CO$ show an apparent p$K$ between 5 and 6 for the $^{13}CO$ NMR shifts (Moon et al., 1977). Proton NMR studies of sperm whale $Mb^{II}O_2$ indicate distal histidine protonation with a p$K$ of 5.7 (Ohms et al., 1979) while for $Mb^{II}CO$ the value is reported to be 5.2 ± 0.2 (Bradbury et al., 1979). The results of temperature-jump measurements on sperm whale $Mb^{III}$-imidazole (Goldsack et al., 1966) and absorption measurements on $Mb^{II}CO$ (Hayashi et al., 1976) also suggest that the distal histidine hydrogen bonds to the sixth ligand with a p$K$ of about 5.7. Electric field pulse–relaxation measurements on the rates of ionization of the iron-bound water molecule in metmyoglobin and methemoglobin suggested the existence of a very rapid internal proton-transfer reaction which proceeds through a hydrogen bond to the distal histidine (Ilgenfritz & Schuster, 1971). In addition, EPR studies of sperm whale cobalt $MbO_2$ indicate a p$K$ value of 5.3 for the distal histidine and revealed that there is no pH dependence of the EPR spectrum in *glycera* cobalt $HbO_2$ because of the absence of a distal histidine (Saito et al., 1977). Our observed p$K$ values for distal histidine protonation and hydrogen bonding are also consistent with $^{15}N$ NMR studies of sperm whale $Mb^{III}CN$ (Morishima & Inubushi, 1978).

Another feature of the Raman spectra consistent with the formation of a hydrogen bond to the $F^-$ anion is the appearance

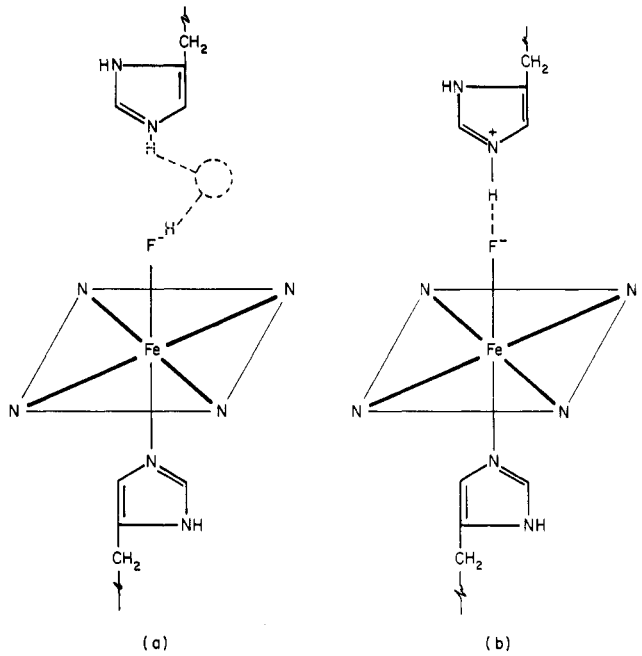


FIGURE 8: Heme geometry of $Hb^{III}F$ and $Mb^{III}F$. (a) pH,7.0. The fluoride anion is bound to the heme iron. About half of the heme cavities contain a water molecule hydrogen bonded to the fluoride anion. This partial $H_2O$ occupancy is indicated by the dashed $H_2O$ moiety. The non-hydrogen-bonded Fe–F stretching vibration occurs at 461 (468) cm$^{-1}$ in $Mb^{III}F$ ($Hb^{III}F$), while the water hydrogen-bonded Fe–F stretching vibration occurs at 421 (439) cm$^{-1}$ in $Mb^{III}F$ ($Hb^{III}F$). (b) pH <6.0. The distal histidine protonates and hydrogen bonds directly to the $F^-$, lowering the Fe–F stretching frequency to 399 (407) cm$^{-1}$ in $Mb^{III}F$ ($Hb^{III}F$).

of intense overtones for the 399- ($Mb^{III}F$) and 407-cm$^{-1}$ Raman peaks. These features are evident at ca. 790 and 800 cm$^{-1}$ in the Raman spectra shown in Figures 3 and 4 and as troughs in the difference spectra in Figures 5 and 6. The intensities of these peaks increase linearly with the intensity of the 399- ($Mb^{III}F$) and 407-cm$^{-1}$ ($Hb^{III}F$) peaks. A much lower intensity is observed for the 934- and 920-cm$^{-1}$ overtones of the non-hydrogen-bonded 468- and 461-cm$^{-1}$ Fe–F stretching fundamentals in $Hb^{III}F$ (Figure 3) and $Mb^{III}F$ (Figure 4), respectively.

Vibrational overtones in Raman spectra can result from anharmonicities in the electronic potential function (Herzberg, 1945). An increased anharmonicity for the Fe–F stretching vibrational potential function would occur due to hydrogen

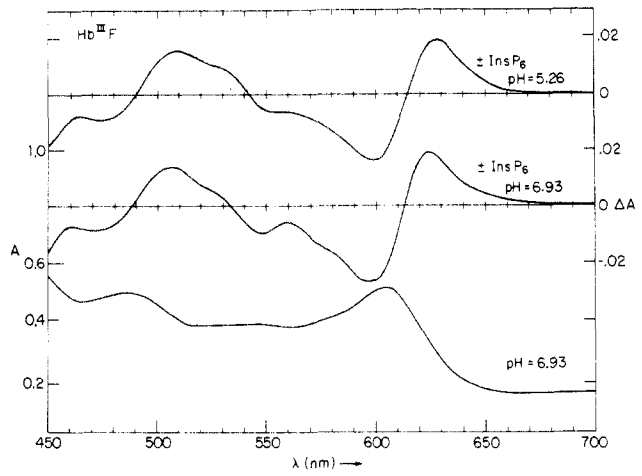


FIGURE 9: Inositol hexaphosphate difference spectrum for methemoglobin fluoride at pH 6.93 and 5.26. $Hb^{III}F$ concentration = 42 $\mu$M heme in 0.1 M KF and 0.025 M buffer ($KPO_4^{2-}$ pH 6.93, and sodium acetate, pH 5.26). Path length = 1 cm; $T$ = 20 °C. pH values after addition of saturating amounts of $InsP_6$ were 7.35 and 5.59.

bonding between the fluoride and the distal histidine proton. This interaction would decrease the curvature of the potential energy well for Fe–F bond lengths greater than the equilibrium diatomic separation. The increased overtone intensity could also result from an increased equilibrium distance difference between the ground- and excited-state potential minima for the hydrogen-bonded species (Clark & Stewart, 1979).

The p$K$ of any particular amino acid residue depends upon numerous factors, including solvent accessibility, environmental dielectric constant, local charge distribution, and intermolecular interactions between the residue and adjacent amino acid. This environmental dependence is clearly evident from the 0.4 pH difference observed for the p$K$ values of the distal histidines in $Mb^{III}F$ and $Hb^{III}F$. As a result, p$K$ measurements of a particular amino acid can be used to probe amino acid environment and protein conformation [Friend & Gurd (1979) and references cited therein]. We have examined the effect of allosteric conformational changes on both the p$K$ of the $Hb^{III}F$ distal histidine and the force constant of the distal histidine–hydrogen-bonded fluoride–iron stretching frequency.

The absorption spectral data shown in Figure 9 indicate that $InsP_6$ converts $Hb^{III}F$ from the R to the T quaternary form both at neutral pH (Perutz et al., 1974b,c) and at pH values where approximately 50% of the distal histidines are protonated; Figure 9 shows the ±$InsP_6$ absorption difference spectra of $Hb^{III}F$ solutions at pH 7.0 and pH 5.0. The only significant change between the pH 7.0 and pH 5.0 difference spectrum is that all of the features in the pH 7.0 difference spectrum shift ca. 15 Å to a longer wavelength in response to the corresponding shift of the pH 5.0 absorption spectrum. The UV absorption spectral changes induced by $InsP_6$ in the pH 5.0 sample are similar to those observed at neutral pH (Perutz et al., 1974 a–c), again suggesting that $InsP_6$ has induced the R to T conversion in the pH 5.0 sample.

Raman and absorption spectral measurements of the pH dependence of samples with and without $InsP_6$ show little or no difference in the distal histidine p$K$ values (±0.15) nor in the frequencies (±1.0 cm) or intensities (±5%) of the Fe–F stretching vibrations. This result is similar to our recent observation at neutral pH, that shifts in the frequency of the Fe–F vibrations induced by $InsP_6$ are limited to less than ±0.5 $cm^{-1}$ (Asher & Schuster, 1981a,b).

## Discussion and Conclusions

Although direct hydrogen bonding from the distal histidine to the axial ligand was suggested by the crystal structure analysis of metmyoglobin azide (Stryer et al., 1964), unambiguous characterization of such bonding in solution has proved to be elusive. The 60-$cm^{-1}$ shift to lower frequency of the Fe–F stretching vibrations in $Hb^{III}F$ and $Mb^{III}F$ at acid pH found in the present study is interpreted to result from protonation of the distal histidine and formation of a hydrogen bond to the fluoride ligand. Since the $F^-$ is ionically bound to the iron and the Fe–F stretch is a diatomic vibration (Asher & Schuster, 1979, 1981a,b), a decreased net charge on the fluoride atom leads to a smaller vibrational stretching force constant, a decreased Fe–F stretching frequency, and an increased bond length.

We recently examined the absorption and resonance Raman spectra of $Hb^{III}F$, and its isolated subunits, and of $Mb^{III}F$ and noted that a decrease in the the Fe–F stretching frequency correlates with an increased wavelength maximum for the ca. 6000-Å absorption band (Asher & Schuster, 1981a,b). The Fe–F frequency differences were interpreted to result from elongations of the Fe–F bonds in the series $Mb^{III}F > \alpha$ subunits $> \beta$ subunits, induced by an increased out-of-plane displacement of the iron to the proximal heme side. An elongation of the Fe–F bond results in a decreased repulsive interaction between the fluoride ligand and those electrons occurring within the iron d orbitals populated in the charge-transfer electronic transition responsible for the 6000-Å absorption band. The resulting decrease in the energy of the excited state leads to a shift of the absorption band to a longer wavelength. A larger shift to a longer wavelength would be expected from the decrease in the effective charge on a hydrogen-bonded fluoride ligand.

Absorption spectral shifts of charge-transfer absorption bands to longer wavelengths upon hydrogen bonding of the distal histidine should be a general phenomena for ionically bound ligands. A previous study of the pH dependence of the visible absorption spectrum of deoxymyoglobin and (carbon monoxy)myoglobin (Hayashi et al., 1976) indicated spectral changes with apparent p$K$ values of 5.6 and 5.7, respectively. The spectra of these ferrous proteins were found to be blue shifted in both cases as the solution pH was decreased, in contrast to our observations on ferric derivatives. However, in the case of $O_2$ and CO ligands, which are covalently bound, the effect of distal histidine hydrogen bonding on the *heme* $\pi \rightarrow \pi^*$ absorption bands is more complex and difficult to predict.

It is likely that pH-dependent absorption spectral measurements could serve as a useful method for examining the p$K$ of distal histidine groups in various hemoglobins and myoglobins. However, care must be exercised to prevent interference from ligand-substitution spectral changes.

The present results should not be taken to infer that no other amino acid side chains in hemoglobin or myoglobin titrate in the pH 5 range. For example, both NMR measurements and theoretical calculations indicate a p$K$ value of 5.4 for histidine-119 in sperm whale myoglobin (Botelho & Gurd, 1978; Botelho et al., 1978). However, the optical and Raman titration data obtained from pH 9 to 5 suggest only one p$K$ value is associated with the observed spectral changes.

Studies on mutant hemoglobins suggest that distal histidine residues interact sterically and electronically with carbon monoxide but not with oxygen in the ferrous derivatives (Tucker et al., 1978), thus leading to a change in the $CO/O_2$ partition coefficient when the distal histidine is absent. Recent kinetic and equilibrium studies on a histidine-chelated protoheme model compound in micelles indicate that the prop-

erties of R-state ferrous hemoglobin can be simulated rather closely in the absence of a distal histidine residue (Traylor & Berzinis, 1980). However, Traylor & Berzinis (1980) also summarized data showing that distal steric effects must be present in myoglobins. Clearly, the quantitative influence of distal heme residues is incompletely understood. The properties of myoglobins or hemoglobins which lack a distal histidine are considerably altered from those that do, as in the case of *glycera* hemoglobin which lacks a distal histidine and has a substantially reduced affinity for all ligands as compared with other single-chain hemoglobins (Seamonds, 1971). Thus, these spectroscopic measurements of p$K$ values are useful for detailing features of the interactions between the heme, its ligand, and the globin.

From recent detailed studies, it is clear that globin amino acid p$K$ values depend on the amino acid environment (Botelho & Gurd, 1978; Botelho et al., 1978; Wilbur & Allerhand, 1977; Matthew et al., 1979; Shire et al., 1974a,b, 1975). The observation that the difference in the distal histidine pK value is less than 0.2 between the R and T forms of $Hb^{III}F$ and the lack of a shift in the distal histidine–hydrogen-bonded fluoride–iron stretching frequency suggest that no major movement of the distal histidine occurs relative to the heme plane upon the R to T conversion in $Hb^{III}F$. It is difficult to estimate the dependence of the hydrogen-bonded Fe–F stretching *frequency* on the distance between the fluoride ion and the histidine. However, the dependence of the distal histidine *pK value* upon the distance from the iron and fluoride atoms can be roughly estimated by considering a simplified electrostatic model which neglects all electrostatic interactions except those between the histidine side chain and the iron and fluoride atoms (the closest charged groups):

$$\frac{\partial \mathrm{p}K}{\partial r} = \frac{-e^2}{2.303kTD}\left(\frac{1}{r^2} - \frac{1}{(r+\Delta)^2}\right)$$

where $e$ is the unit electronic charge on the fluoride and iron atoms and $k$, $T$, and $D$ are the Boltzman constant, temperature, and dielectric constant, respectively. With the assumption of point charges, $r$ is the distance between the $F^-$ anion and the histidine, and $r + \Delta$ is the distance of the iron from the distal histidine. For $D = 4$, $r = 3$ Å, and $\Delta = 2.3$ Å, we can estimate $\partial \mathrm{p}K/\partial r = 0.1$ p$K$ unit/0.1-Å distal histidine movement relative to the iron and fluoride ions. This estimate of the heme–histidine distance p$K$ dependence suggests that any movement of the distal histidine from the fluoride ligand between the R and T quaternary forms is limited to <0.2 Å.

The spectroscopic data reported here show that the ultraviolet and visible absorbance changes seen in methemoglobin upon addition of $InsP_6$ result from changes in heme–globin nonbonded interactions and not from changes in heme–axial ligand bonding. The constancy of the Fe–F bond length in the two quaternary forms of methemoglobin fluoride is in agreement with the results of Nagai et al. (1980), who found that the Fe–$O_2$ bond length in oxyhemoglobin is the same in both R and T forms of the protein. The lack of correspondence between absorption spectral shifts previously thought diagnostic of iron movement from the heme plane (Perutz et al., 1974a–c) and changes in the Fe–F bond length indicate that any conclusions concerning the cooperativity mechanism based on absorption spectral data should be reexamined.

## Acknowledgments

We gratefully acknowledge the helpful conversations with Margaret Flanagan (Chemistry Department, Indiana University, Bloomington, IN) and the assistance of Dr. Steven Shire in providing a computer program for evaluation of the titration data.

## References

Asher, S., & Sauer, K. (1976) *J. Chem. Phys. 64*, 4115.
Asher, S. A., & Schuster, T. M. (1979) *Biochemistry 18*, 5377.
Asher, S. A., & Schuster, T. M. (1981a) in *Interaction Between Iron and Proteins in Oxygen and Electron Transport* (Ho, C., Ed.) Elsevier, New York.
Asher, S. A., & Schuster, T. M. (1981b) *Biochemistry* (in press).
Asher, S. A., Vickery, L. E., Schuster, T. M., & Sauer, K. (1977) *Biochemistry 16*, 5849.
Beetlestone, J. G., & Irvine, D. H. (1968) *J. Chem. Soc. A*, 960.
Beetlestone, J. G., & Irvine, D. H. (1969) *J. Chem. Soc. A*, 735.
Botelho, L. H., & Gurd, F. R. N. (1978) *Biochemistry 17*, 5188.
Botelho, L. H., Friend, S. H., Matthew, J. B., Lehman, L. D., Hanania, G. I. H., & Gurd, F. R. N. (1978) *Biochemistry 17*, 5197.
Bradbury, J. H., Deacon, S. L. M., & Ridgway, M. D. (1979) *J. Chem. Soc., Chem. Commun.*, 998.
Churg, A. K., Glick, H. A., Zelano, J. A., & Makinen, M. W. (1980) in *Biological and Clinical Aspects of Oxygen* (Caughey, W. S., Ed.) p 125, Academic Press, New York.
Clark, R. J. H., & Stewart, B. (1979) *Struct. Bonding (Berlin) 36*, 1.
Deatherage, J. F., Loe, R. S., & Moffat, K. (1976) *J. Mol. Biol. 104*, 723.
Eaton, W. A., & Hochstrasser, R. M. (1968) *J. Chem. Phys. 49*, 985.
Fabry, M. E., & Eisenstadt, M. (1974) *J. Biol. Chem. 249*, 2915.
Fermi, G., & Perutz, M. F. (1977) *J. Mol. Biol. 114*, 421.
Friend, S. H., & Gurd, F. R. N. (1979) *Biochemistry 18*, 4612.
Goldsack, D. E., Eberlin, W. S., & Alberty, R. A. (1966) *J. Biol. Chem. 241*, 2653.
Gupta, R. K., & Mildvan, A. S. (1975) *J. Biol. Chem. 250*, 246.
Hayashi, Y., Yamada, H., & Yamazaki, I. (1976) *Biochim. Biophys. Acta 427*, 468.
Herzberg, G. (1945) *Infrared and Raman Spectra of Polyatomic Molecules*, Van Nostrand-Reinhold, New York.
Ilgenfritz, G., & Schuster, T. M. (1971) in *Probes of Structure and Function of Macromolecules and Membranes, Vol. II* (Chance, B., Yonetani, T., & Mildvan, A., Eds.) Academic Press, New York.
Kitagawa, T., Kyogoku, Y., Iizuka, T., & Saito, M. I. (1976) *J. Am. Chem. Soc. 98*, 5169.
Koenig, S. H., Brown, R. D., & Lindstrom, T. R. (1981) in *Interaction Between Iron and Proteins in Oxygen and Electron Transport* (Ho, C., Ed.) Elsevier, New York.
Matthew, J. B., Hanania, G. I. H., & Gurd, F. R. N. (1979) *Biochemistry 18*, 1919.
Moffat, K., Deatherage, J. F., & Seybert, D. W. (1979) *Science (Washington, D.C.) 206*, 1035.
Moon, R. B., Dill, K., & Richards, J. H. (1977) *Biochemistry 16*, 221.
Morishima, I., & Inubushi, T. (1978) *J. Am. Chem. Soc. 100*, 3568.
Nagai, K., Kitagawa, T., & Morimoto, H. (1980) *J. Mol. Biol. 136*, 271.
Ohms, J. P., Hagenmaier, H., Hayes, M. B., & Cohen, J. S. (1979) *Biochemistry 18*, 1599.

Perutz, M. F. (1979) *Annu. Rev. Biochem. 48*, 327.
Perutz, M. F., Ladner, J. E., Simon, S. R., & Ho, C. (1974a) *Biochemistry 13*, 2163.
Perutz, M. F., Fersht, A. R., Simon, S. R., & Roberts, G. C. K. (1974b) *Biochemistry 13*, 2174.
Perutz, M. F., Heidner, E. J., Ladner, J. E., Beetlestone, J. G., Ho, C., & Slade, E. F. (1974c) *Biochemistry 13*, 2187.
Perutz, M. F., Sanders, J. K. M., Chenery, D. H., Noble, R. W., Pennelly, R. R., Fung, L. W.-M., Ho, C., Giannini, I., Pörschke, D., & Winkler, H. (1978) *Biochemistry 17*, 3640.
Saito, M. I., Iizuka, T., Yamamoto, H., Kayne, F. J., & Yonetani, T. (1977) *J. Biol. Chem. 252*, 4882.
Seamonds, B. (1971) in *Probes of Structure and Function of Macromolecules* (Chance, B., Yonetani, T., & Mildvan, A. S., Eds.) p 317, Academic Press, New York.
Shire, S. J., Hanania, G. I. H., & Gurd, F. R. N. (1974a) *Biochemistry 13*, 2967.
Shire, S. J., Hanania, G. I. H., & Gurd, F. R. N. (1974b) *Biochemistry 13*, 2974.
Shire, S. J., Hanania, G. I. H., & Gurd, F. R. N. (1975) *Biochemistry 14*, 1352.
Smith, D. W., & Williams, R. J. P. (1970) *Struct. Bonding (Berlin) 7*, 1.
Spiro, T. G. (1975) *Biochim. Biophys. Acta 416*, 169.
Spiro, T. G., & Burke, J. M. (1976) *J. Am. Chem. Soc. 98*, 5482.
Stryer, L., Kendrew, J. C., & Watson, H. C. (1964) *J. Mol. Biol. 8*, 96.
Theorell, H., & Ehrenberg, A. (1951) *Acta Chem. Scand. 5*, 823.
Traylor, T. G., & Berzinis, A. P. (1980) *Proc. Natl. Acad. Sci. U.S.A. 77*, 3171.
Tucker, P. W., Phillips, S. E. V., Perutz, M. F., Houtchens, R., & Caughey, W. S. (1978) *Proc. Natl. Acad. Sci. U.S.A. 75*, 1076.
Vickery, L., Nozawa, T., & Sauer, K. (1976) *J. Am. Chem. Soc. 98*, 343.
Wilbur, D. J., & Allerhand, A. (1977) *J. Biol. Chem. 252*, 4968.
Zerner, M., Gouterman, M., & Kobayashi, H. (1966) *Theor. Chim. Acta 6*, 363.

# pH Dependence of the High-Resolution Proton Nuclear Magnetic Resonance Spectrum of the *lac* Repressor Headpiece†

A. A. Ribeiro, D. Wemmer, R. P. Bray, and O. Jardetzky*

ABSTRACT: The pH dependence of the N-terminal 51 amino acid headpiece (HP) of the *lac* repressor has been followed by using $^1$H NMR spectroscopy to monitor the chemical shifts of resolved aromatic and methyl resonances. The NMR evidence reveals the folded HP domain to be stable from pH 1 to 10 at 23 °C. All observed resonances shift toward their expected random-coil positions above pH 10, which suggests that a general unfolding occurs. The four tyrosine rings reflect a combination of unfolding and titration in the order 7 > 17, 12 > 47. This pH-induced unfolding is completely reversible. In addition, strikingly similar pH behavior for selected tyrosine and methyl resonances at acid pH values suggests that clusters of various tyrosine, methyl, and carboxyl side chains exist in the native structure.

The isolated N-terminal portion of the *lac* repressor protein, termed "headpiece" (HP), has been shown to have a strong affinity for double-helical deoxyribonucleic acid (DNA) (Geisler & Weber, 1977) and to bind to *lac* operator DNA (Ogata & Gilbert, 1978, 1979). The specific binding of whole repressor to *lac* operator DNA controls the lactose genes in *Escherichia coli*. Studies of the structural properties of the HP are therefore of intrinsic interest to questions about genetic control.

No crystals of the HP or repressor suitable for high-resolution X-ray studies are yet available. $^1$H NMR (Wade-Jardetzky et al., 1979; Buck et al., 1978) and low-angle X-ray studies (Pilz et al., 1980) suggest that the HP forms an independent structural domain whether it is part of the complete repressor or separated from a core domain by proteolytic cleavage. The HP (amino acids 1–51) appears connected to the core (amino acids 60–360) by a flexible hinge localized between residues 50 and 60. The flexible hinge allows the HP DNA-binding domain to have a high degree of motion with respect to the core. Many $^1$H NMR resonances observable in the native isolated HP are similarly observed in the intact repressor (Wade-Jardetzky et al., 1979).

The 360-MHz $^1$H NMR spectrum of isolated HP-51 reflects extensive folded structure. The resolution and initial analysis of a considerable number of $^1$H resonances in the aromatic and aliphatic regions described in previous papers (Ribeiro et al., 1981a,b) allow the use of those resonances as natural probes of the HP structure. Thus, the temperature-induced unfolding of the HP was reported (Wemmer et al., 1981a). Unlike most proteins thus far investigated, this small single-chain polypeptide which possesses no disulfide bridges was found to unfold with weak cooperativity. The thermal denaturation occurs in a gradual and continuous manner in which native and partially unfolded structures are in rapid exchange, and the process appears completely reversible (Wemmer et al., 1981a).

Given the important DNA-binding role of the HP, and its unusual thermal unfolding properties, we have now investigated the effects of pH on the protein structure. In this paper, we consider the phenomena observed in the aromatic and aliphatic

† From the Stanford Magnetic Resonance Laboratory, Stanford University, Stanford, California 94305. *Received December 9, 1980.* This is paper 4 in the series High-Resolution NMR Studies of the *lac* Repressor. This research was supported by grants from the National Institutes of Health (GM18098 and RR00711) and from the National Science Foundation (GP23633).

0006-2960/81/0420-3346$01.25/0 